Toxicology 314 (2013) 174–182

Contents lists available at ScienceDirect

Toxicology

journal homepage: www.elsevier.com/locate/toxicol

# Acute iron overload and oxidative stress in brain

Natacha E. Piloni[a], Virginia Fermandez[b], Luis A. Videla[b], Susana Puntarulo[a,*]

[a] Physical Chemistry-Institute of Biochemistry and Molecular Medicine (IBIMOL), School of Pharmacy and Biochemistry, University of Buenos Aires-CONICET, Buenos Aires, Argentina
[b] Molecular and Clinical Pharmacology Program, Institute of Biomedical Sciences, Faculty of Medicine, University of Chile, Santiago, Chile

ARTICLE INFO

*Article history:*
Received 27 July 2013
Received in revised form 9 September 2013
Accepted 30 September 2013
Available online xxx

*Keywords:*
Brain
oxidative stress
Iron
Free radicals
NF-κB
EPR

ABSTRACT

An *in vivo* model in rat was developed by intraperitoneally administration of Fe-dextran to study oxidative stress triggered by Fe-overload in rat brain. Total Fe levels, as well as the labile iron pool (LIP) concentration, in brain from rats subjected to Fe-overload were markedly increased over control values, 6 h after Fe administration. In this *in vivo* Fe overload model, the ascorbyl ($A^{\bullet}$)/ascorbate ($AH^{-}$) ratio, taken as oxidative stress index, was assessed. The $A^{\bullet}/AH^{-}$ ratio in brain was significantly higher in Fe-dextran group, in relation to values in control rats. Brain lipid peroxidation indexes, thiobarbituric acid reactive substances (TBARS) generation rate and lipid radical ($LR^{\bullet}$) content detected by Electron Paramagnetic Resonance (EPR), in Fe-dextran supplemented rats were similar to control values. However, values of nuclear factor-kappaB deoxyribonucleic acid (NFκB DNA) binding activity were significantly increased (30%) after 8 h of Fe administration, and catalase (CAT) activity was significantly enhanced (62%) 21 h after Fe administration. Significant enhancements in Fe content in cortex (2.4 fold), hippocampus (1.6 fold) and striatum (2.9 fold), were found at 6 h after Fe administration. CAT activity was significantly increased after 8 h of Fe administration in cortex, hippocampus and striatum (1.4 fold, 86, and 47%, respectively). Fe response in the whole brain seems to lead to enhanced NF-κB DNA binding activity, which may contribute to limit oxygen reactive species-dependent damage by effects on the antioxidant enzyme CAT activity. Moreover, data shown here clearly indicate that even though Fe increased in several isolated brain areas, this parameter was more drastically enhanced in striatum than in cortex and hippocampus. However, comparison among the net increase in $LR^{\bullet}$ generation rate, in different brain areas, showed enhancements in cortex lipid peroxidation, without changes in striatum and hippocampus $LR^{\bullet}$ generation rate after 6 h of Fe overload. This information has potential clinical relevance, as it could be the key to understand specific brain damage occurring in conditions of Fe overload.



## 1. Introduction

Several pathological conditions are currently associated with iron (Fe) overload. Clinical and epidemiologic observations indicate that increased Fe storage status is a risk factor in several diseases, such as porphyria cutanea tarda and the sudden infant death syndrome (Puntarulo, 2005). Hepatotoxicity is the most consistent finding in patients with Fe overload, followed by cardiac disease, endocrine abnormalities, arthropathy, osteoporosis, and skin pigmentation (Galleano and Puntarulo, 1994). Fe excess generates oxidative stress. Superoxide anion ($O_2^{-}$) and hydrogen peroxide ($H_2O_2$) toxicity arises from their Fe-dependent conversion into the extremely reactive hydroxyl radical ($^{\bullet}OH$) (Haber–Weiss reaction) generating severe damage to membranes, proteins, and deoxyribonucleic acid (DNA) (Halliwell and Gutteridge, 1984). Different protocols of Fe treatments in the rat, supplemented either in the diet or intraperitoneally (ip) injected, lead to a specific profiles in Fe content deposition in several tissues and plasma (Piloni and Puntarulo, 2010). Fe-dextran treatment, primarily affecting the liver, constitutes a good model for Fe toxicity evaluation, as it leads to similar pathological and clinical consequences observed after acute Fe overload in humans (Puntarulo, 2005). In the rat, we have developed an *in vivo* model consisting of ip Fe-dextran administration, followed by excision of the organ after 6 h (Galleano and Puntarulo, 1992). The effect of increasing Fe content in rat brain under this protocol of Fe administration has not been described yet, however, it has been shown to increase liver, kidney and circulating

*Abbreviations:* NF-κB, nuclear factor kappa B; DNA, deoxyribonucleic acid; $A^{\bullet}$, ascorbyl radical; $AH^{-}$, ascorbate; EPR, Electron Paramagnetic Resonance; $LR^{\bullet}$, lipid derived radicals; TBARS, thiobarbituric acid reactive substances; CAT, catalase; $O_2^{-}$, superoxide anion; $O_2$, oxygen; $H_2O_2$, hydrogen peroxide; $^{\bullet}OH$, hydroxyl radical; ROS, reactive oxygen species; LIP, labile iron pool; CA, calcein; TGA, thioglycolique acid; DMSO, dimethyl sulfoxide; TEMPO, 2,2,5,5-tetramethyl piperidine-1-oxyl; PBN, N-t-butyl-α-phenyl nitrone; α-T, alpha tocopherol; DHA, dehydroascorbic acid; SOD, superoxide dismutase; DF, deferoxamine mesylate; Ft, ferritin.

* Corresponding author at: Fisicoquímica-IBIMOL, Facultad de Farmacia y Bioquímica, Junín 956, CAAD1113 Buenos Aires, Argentina. Tel.: +54 11 4964 8244x101; fax: +54 11 4508 3646x102.
*E-mail address:* susanap@ffyb.uba.ar (S. Puntarulo).

0300-483X/$ – see front matter © 2013 Elsevier Ireland Ltd. All rights reserved.
http://dx.doi.org/10.1016/j.tox.2013.09.015

**Table 1**
Fe content and lipid peroxidation after Fe-dextran treatment.

| | Control | Fe-dextran | References |
|---|---|---|---|
| **Liver** | | | |
| Total Fe content (μg/g tissue) | 45 ± 10 | 201 ± 28* (+446%) | (1) |
| TBARS (pmol/min/mg prot) | 40 ± 1 | 110 ± 30* (+175%) | (2) |
| **Kidney** | | | |
| Fe content (μg/g DW) | 14 ± 3 | 113 ± 15* (+707%) | (3) |
| TBARS (pmol/min/mg prot) | 29 ± 2 | 37 ± 3* (+27%) | (3) |
| **Plasma** | | | |
| Fe content (μg/dl) | 126 ± 20 | 1538 ± 158* (+1220%) | (4) |
| TBARS (nmol/ml) | 0.7 ± 0.1 | 2.7 ± 0.1* (+285%) | (4) |
| $A^{\bullet}/AH^{-}$ ratio ($\times 10^{-4}$ AU) | 4 ± 1 | 11 ± 1* (+275%) | (5) |

Acute Fe overload was developed by injecting male Wistar rats with Fe-dextran (500 mg/body wt). Control animals were injected with dextran. Data in liver were taken after 6 h of the Fe administration and data in kidney and plasma after 20 h of Fe supplementation. (1) Galleano et al., 2004; (2) Puntarulo, 2005; (3) Galleano and Puntarulo, 1994; (4) Galleano and Puntarulo, 1995; (5) Galleano et al., 2002.
* Significantly different from control values ($p < 0.01$).

total Fe content, in concomitance with thiobarbituric acid reactive substances (TBARS) generation in those compartments (Table 1). It was suggested that Fe supplied as Fe-dextran is initially taken up by Kupffer cells in the liver, and when their storage capacity is exceeded the metal is accumulated by parenchymal cells producing a mild Fe overload. Interestingly, acute Fe overload alters the Kupffer cell functional status by inducing a progressive enhancement in macrophage-dependent respiratory burst activity at early times after treatment, a process associated with significant production of reactive oxygen species (ROS) (Tapia et al., 1998).

In order to enter the brain, Fe needs to cross two distinct barriers, the blood–brain barrier and the blood–cerebrospinal barrier (Pardridge et al., 1987; Zheng and Monnot, 2012). Fe-related neurodegenerative disorders can result from both Fe accumulation or defects in its metabolism and/or homeostasis (Batista-Nascimento et al., 2012). Brain tissue is thought to be more susceptible to ROS-dependent damage than other organs, a feature associated with (i) the fact that neurons are enriched in mitochondria and possess a rather high aerobic metabolism; (ii) the low levels of some antioxidant enzymes; (iii) the high content of polyunsaturated fatty acids in brain membranes; and (iv) the high Fe content, which may combine their effects to make the brain a preferential target for oxidative stress-related degeneration (Halliwell, 2006). Under physiological conditions, neuronal Fe is not reactive despite its high level, probably because its absorption, transport, and storage are tightly regulated; however, Fe-induced oxidative stress is likely to occur if an excess of ionic Fe is achieved (Floyd and Carney, 1992). Abnormal Fe metabolism can result in human neurologic disorders such as Alzheimer's, Parkinson's, and Huntigton disease (Gerlach et al., 1994). This assumption is supported by reports from Yu et al. (2011) showing that Fe-overload-induced oxidative stress in rats strengthen the complexity of risk assessment of psychological stress, as well as those from Chen et al. (2013) stating that increased $Fe^{2+}$ in the brain, attained by intracerebral ventricular injection of $Fe^{2+}$ induced autophagic cell death. Papanastasiou et al. (2000) reported that Fe uptake by the brain of rats chronically supplemented with Fe-carbonyl or intravenously injected with Fe polymaltose, was not significantly affected. More recently, Maaroufi et al. (2009) developed a chronic Fe overload model consisting in 3 mg Fe/kg, daily administrated to adult rats during 5 days. These treatments resulted in a late (16 days after treatment) and significant Fe accumulation in the hippocampus, the cerebellum, and the basal ganglia. Maaroufi et al. (2011) studies in rats, receiving daily Fe ip injections (3 mg $FeSO_4$/kg) or 0.9% sodium chloride (vehicle) during 21 consecutive days, showed that Fe accumulation correlated with behavioral deficits. However, TBARS content was not increased in different brain areas. This effect was accompanied by enhanced superoxide dismutase (SOD) and catalase (CAT) activities, suggesting that chronic Fe administration may have induced adaptive responses involving stimulation of the antioxidant defense systems. The underlying mechanisms of tissue damage are not clear, and they probably depend on the Fe administration protocol. Even though lipid damage was observed in many cases after Fe overload, antioxidant capacity seems to play a crucial role in controlling the impairment mechanisms.

The aim of the present study was to contribute to the understanding of the complex mechanism(s) triggered by Fe-overload in rat brain by assaying oxidative stress parameters. The kinetics of total Fe content and the labile Fe pool (LIP) were described. Oxidative stress status was estimated by assaying the ascorbyl radical ($A^{\bullet}$) content/ascorbate ($AH^{-}$) ratio and lipid damage as the rate of TBARS generation. EPR detection of lipid radicals ($LR^{\bullet}$) generation, CAT activity and nuclear factor-kappaB deoxyribonucleic acid (NF-κB DNA) binding activity were also evaluated.

## 2. Materials and methods

### 2.1. Animal preparation

Male Sprague-Dawley rats (180 ± 10 g, 45 ± 5 days old), from the Animal Facility of the School of Pharmacy and Biochemistry of the University of Buenos Aires, were used. The animals were housed under standard conditions of light, temperature and humidity with unlimited access to water and food. A single dose of 500 mg/kg body weight Fe-dextran was ip injected. Control rats were sham-injected ip with physiological saline solution. At 1, 2, 4, 6, 8, 21 and 29 h after Fe treatment or some of this time points specified in each experiment, brain was removed from the anesthetized animals in a $CO_2$ chamber. Depending on the protocol, brain cortex, hippocampus and striatum or the whole brain were rapidly removed and immediately frozen and stored under liquid $N_2$. Dissection was performed as described by Czerniczyniec et al. (2011). Experimental animal protocols and animal procedures complied with the Guide for the Care and Use of Laboratory Animals (National Academy of Sciences, NIH Publication 6-23, revised 1985) and according to the principles and directives of the European Communities Council Directives (86/609/EEC). The procedures also received approval from the local ethics committee.

### 2.2. Total Fe content

Brain cortex, hippocampus and striatum and the whole brain were dried in an oven at 60 °C until constant weight, were mineralized in $HNO_3$ according to Laurie et al. (1991). Fe concentration was spectrophotometrically determined after reduction with thioglycolic acid measuring the absorbance at λ = 535 nm in the presence of bathophenanthroline according to Brumby and Massey (1967).

### 2.3. Labile iron pool (LIP)

The LIP was determined by a fluorescence technique with the Fe sensor calcein (CA) according to Darbari et al. (2003) with modifications. Brain samples were homogenized in 2 volumes of 40 mM potassium phosphate buffer, 120 mM KCl, pH 7.4. The homogenate was centrifuged at 10,000 × *g* for 15 min at 4 °C. The supernatant was passed through filters with 30,000 nominal molecular weight limit. The filtered solution was then reduced for 10 min with 1 volume of 8% thioglycolic acid (TGA). Fe in the reduced solution was measured using 1 mM CA solution in 40 mM potassium phosphate buffer, 120 mM KCl, pH 7.4. When Fe is added to CA solution a fraction of the dye binds free $Fe^{2+}$ leading to the generation of the Fe-bound (quenched) form [CA-Fe], while another fraction remains free as unbound calcein [CA] and provides the basal fluorescence. The fluorescence ($\lambda_{exc}$ = 485 nm, $\lambda_{em}$ = 535 nm) was monitored until stabilization of the signal and then deferoxamine mesylate (DF) salt was added to a final concentration of 800 mM. The fluorescence was monitored until a new stabilization of the signal. Then $Fe^{2+}$ + $Fe^{3+}$ concentration was assessed according to Robello et al. (2007).

### 2.4. Detection of $A^{\bullet}$ by Electron Paramagnetic Resonance (EPR)

Over the past decade the EPR detectable concentration of $A^{\bullet}$ has been interpreted either as an index of the transient changes in $AH^{-}$ status (Pietri et al., 1994) or as a reflection of the ongoing free radical flux in the studied system (Jurkiewicz and Buettner, 1994; Galleano et al., 2002). Measurements were performed at room temperature in a Brucker (Karlsruhe, Germany) espectrometer EMX plus Banda X. Brain tissue was homogenized in dimethyl sulfoxide (DMSO) and immediately transferred to a Pasteur pipette for $A^{\bullet}$ detection. Instrument settings were as follows: modulation frequency 500 kHz, microwave power 10 mW, microwave frequency 9.75 GHz, centered field 3520 G, time constant 40.96 ms, modulation amplitude 1 G and sweep

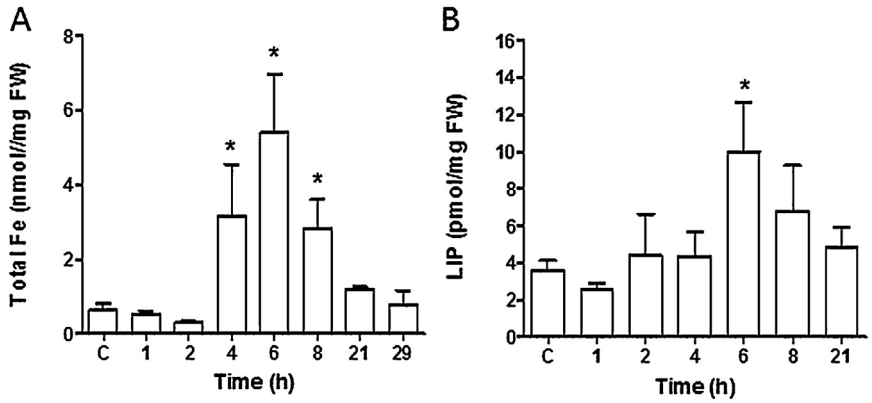


**Fig. 1.** Kinetic study of Fe content in brain. (A) Total Fe content. (B) LIP content in rat brain homogenates in control and Fe-overloaded rats. *Significantly different from control values, ANOVA, $p < 0.05$.

width 15,000 G. Quantification of the spin adduct was performed using an aqueous solution of 2,2,5,5-tetramethyl piperidine-1-oxyl (TEMPO) introduced into the same sample cell used for spin trapping. EPR spectra for both sample and TEMPO solutions were recorded at exactly the same spectrometer settings and the first derivative EPR spectra were double integrated to obtain the area intensity, then the concentration of spin adduct was calculated according to Kotake et al. (1996).

### 2.5. $AH^-$ content

The content of $AH^-$ was measured by reverse phase HPLC with electrochemical detection. Brain samples were homogenized in metaphosphoric acid 10% (w/v) according to Kutnink et al. (1987).

### 2.6. Detection of $LR^\bullet$ generation by EPR

$LR^\bullet$ were detected by a spin trapping technique using N-t-butyl-α-phenyl nitrone (PBN). A 40 mM PBN stock solution was prepared in DMSO immediately prior to use. Brain tissue was homogenized in DMSO-PBN (stock solution), incubated 30 min and immediately transferred to a Pasteur pipette for $LR^\bullet$ detection. Instrument settings were as follows: modulation frequency 50 kHz, microwave power 10 mW, microwave frequency 9.75 GHz, centered field 3487 G, time constant 81.92 ms, modulation amplitude 1.20 G and sweep width 100,000 G, according to Lai et al. (1986). Quantification of the spin adduct was performed using TEMPO introduced into the same sample cell used for spin trapping. EPR spectra for both sample and TEMPO solutions were recorded at exactly the same spectrometer settings and the first derivative EPR spectra were double integrated to obtain the area intensity, then the concentration of spin adduct was calculated according to Kotake et al. (1996).

### 2.7. Content of TBARS

TBARS content was measured using a modified fluorescence method (Boveris and Puntarulo, 1998). An aliquot (50 mg) of brain samples were homogenized with 1 ml of 40 mM potassium phosphate buffer, 120 mM KCl (pH 7.4). To 0.1 ml of homogenate, 0.05 ml of 4% (w/v) butylated hydroxytoluene (BHT) and 0.25 ml 3% sodium dodecyl sulfate were added. After mixing, 1 ml of 0.1 N HCl, 0.15 ml of 10% (w/v) phosphotungstic acid, and 0.5 ml of 0.7% (w/v) 2-thiobarbituric acid was added. The mixture was heated for 45 min in boiling water, and TBARS were extracted into 1 ml of *n*-butanol. After a brief centrifugation, the fluorescence of the butanol layer was measured at $\lambda_{ex} = 515$ nm and $\lambda_{em} = 555$ nm. The values were expressed as nmol TBARS (malondialdehyde equivalents) per mg of protein. Malondialdehyde standards were prepared from 1,1,3,3-tetramethoxypropane.

### 2.8. CAT activity assay

Tissues were homogenized in 40 mM potassium phosphate buffer, 120 mM KCl (pH 7.4) and centrifuged at 600 × *g* for 10 min to obtain the supernatant. CAT activity was assayed spectrophotometrically by the decomposition of $H_2O_2$ at $\lambda = 240$ nm in a reaction mixture consisting of 50 mM potassium phosphate buffer (pH 7.0) containing 10 mM $H_2O_2$ (Aebi, 1984). Protein was determined as described by Lowry et al. (1951).

### 2.9. Lipid soluble antioxidants

The content of α-tocopherol (α-T) in the brain homogenates was quantified by reverse-phase HPLC with electrochemical detection using a Bioanalytical Systems (West Lafayette, IN, USA) LC-4C amperometric detector with a glassy carbon working electrode at an applied oxidation potential of 0.6 V (Desai, 1984). D,L-α-T (Sigma) was used as standard.

### 2.10. Assessment of NF-κB DNA binding

For these studies nuclear protein extracts from brain samples obtained at 4, 6 and 8 h after Fe-dextran injection, were prepared according to Deryckere and Gannon (1994). Brain samples (100–500 mg), frozen in liquid $N_2$ were homogenized in buffer (pH 7.9) with 10 mM HEPES, 1 mM EDTA, 0.6% Nonidet P-40, 150 mM NaCl, and the protease inhibitors (1 mM phenylmethylsulfonyl fluoride, 1 μg/ml aprotinin, 1 μg/ml leucopeptin, and 1 mM orthovanadate). For the determinations homogenates were incubated on ice for 15 min and centrifuged at 4 °C at 100 × *g* for 10 min. Pellets were resuspended in hypotonic buffer and incubated for 15 min on ice. Then, 50 μl of 10% Nonidet P-40 were added and the samples were centrifuged at 14,000 × *g* for 30 s. The precipitate was resuspended in 50 μl extraction buffer, vortexed for 15 s and gently agitated on a platform for 15 min. Then, the samples were centrifuged at 14,000 × *g* during 10 min. The supernatant contains the nuclear fraction of the samples. NF-κB DNA binding was determined by the Protocol NF-kB (Human p50/p60) Combo Transcription Factor Assay Kit, assessing NF-κB DNA binding at $\lambda = 450$ nm.

### 2.11. Light microscopy

Brain tissues from all rats were fixed for 24 h in 10% formalin. Tissues were embedded in paraffin, sectioned (4 μm) and dyed with commonly used stains, hematoxylin and eosin, in order to determine treatment-induced injury (Vázquez et al., 2013).

### 2.12. Statistical analyses

Unless otherwise indicated, data in the text and tables are expressed as mean ± standard error of the media (S.E.M.) of three to five independent experiments, with two replicates in each experiment. Statistical tests were carried out using Graph InStat, Student's *t* test or one-way ANOVA followed by the Newman–Keuls test.

## 3. Results

### 3.1. Effect of Fe-dextran supplementation on Fe brain concentration

Since the kinetic profile of the incorporation of Fe to the brain after Fe-dextran administration has not been described previously, total brain Fe levels were assessed at several time points (1–29 h) after Fe supplementation. Even though total Fe concentration was significantly higher, as compared to control values, at 4, 6, and 8 h pi, a maximum was recorded at 6 h pi (8.5-fold) (Fig. 1A). The LIP concentration was significantly elevated only at 6 h pi (2.5-fold) (Fig. 1B), returning to control values afterwards. However, morphological characteristics of the brain, assessed by light microscopy did not show any significant alteration as compared to control brains at any tested times (data not shown).

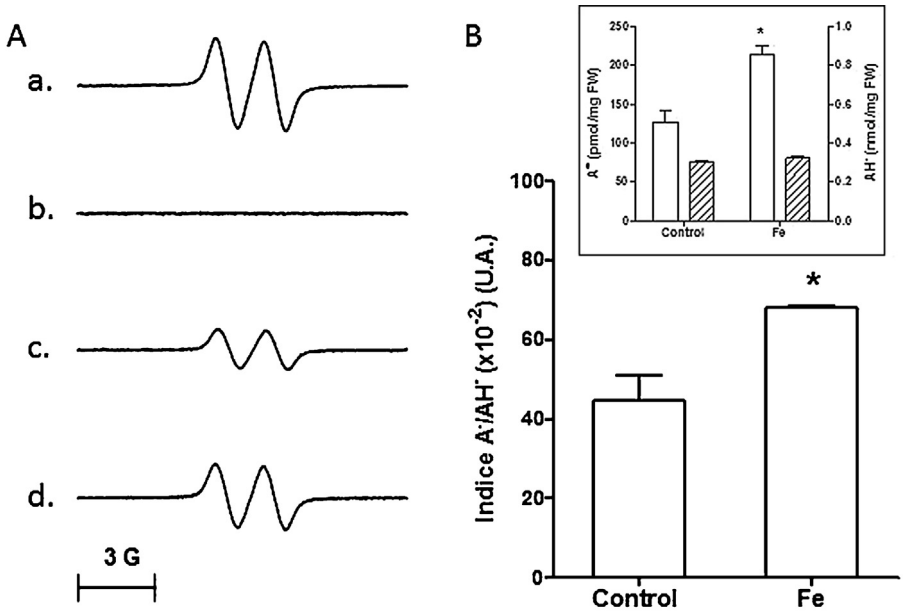


**Fig. 2.** $A^{\bullet}/AH^{-}$ ratio in rat brain. (A) EPR signal for $A^{\bullet}$ in rat brain, (a) computer simulated-spectrum employing the following spectral parameters: $g = 2.005$ and $a_{H^+} = 1.8$ G, (b) DMSO alone, (c) control rat brain, (d) Fe-overloaded rat brain at 6 h pi. (B) $A^{\bullet}/AH^{-}$ ratio in control and Fe-overloaded rat brain at 6 h pi. Insert: $A^{\bullet}$ content (□), $AH^{-}$ content (▨) in control and Fe-overloaded brains. *Significantly different from control values, Student's $t$ test, $p < 0.05$.

### 3.2. Effect of Fe-dextran supplementation on oxidative stress

Since both, total Fe and the LIP concentration, were increased after 6 h of Fe administration, oxidative stress in the hydrophilic cellular medium was evaluated. Fig. 2A shows the typical EPR spectrum of $A^{\bullet}$ in brain from control rats, with the characteristic two lines at $g = 2.005$ and $a_{H^+} = 1.8$ G. $A^{\bullet}$ content in brain samples from control rats was slightly increased after Fe-dextran administration (Fig. 2B, insert). Based on the active metabolism of $AH^{-}$ in rats, it was considered the need for improving the selection of an index to assess oxidative stress in brain under these experimental conditions. Fe-dextran administration did not affect $AH^{-}$ content in brain (Fig. 2B, insert). The $A^{\bullet}/AH^{-}$ ratio under the *in vivo* Fe overload conditions in brain was significantly higher in Fe-dextran treated rats as compared to values in brain from control rats (Fig. 2B), suggesting the development of oxidative stress in the hydrophilic medium under these experimental conditions of treatment.

### 3.3. Effect of Fe-dextran supplementation on lipid peroxidation and membrane antioxidants

The lipid peroxidation, assessed as TBARS content in brain homogenates from control and 6 h Fe-dextran treated animals, was not significantly affected (controls, $0.13 \pm 0.01$; Fe-treated, $0.17 \pm 0.02$ nmol MDA/mg FW). On other hand, $LR^{\bullet}$ combined with the spin trap PBN resulted in adducts that gave a characteristic EPR spectrum with hyperfine coupling constants of $a_N = 15.8$ G and $a_H = 2.6$ G, in agreement with computer simulated signals obtained using those parameters (Fig. 3). Even though these constants could be assigned to lipid radicals, spin trapping studies cannot readily distinguish between $ROO^{\bullet}$, $RO^{\bullet}$ and $R^{\bullet}$ adducts, owing to the similarity of the corresponding coupling constants (Buettner, 1987). PBN itself was examined and no PBN spin adduct was observed (Fig. 3A). Data in Fig. 3B show that even though total Fe concentration (increased after 6 and 8 h pi) and LIP (increased after 6 h) were significantly enhanced as compared to control values, the generation rate of $LR^{\bullet}$ adducts by isolated membranes was not significantly affected at neither of the indicated time points in the brain homogenates.

The concentration of α-T seems a relevant estimation of antioxidant protection at the lipophilic level. Fe overload in brain did not significantly affect the lipid soluble antioxidant concentration ($11.30 \pm 0.05$ and $12.40 \pm 0.07$ pmol/mg FW, for control and 6 h Fe-dextran treated animals, respectively).

### 3.4. Effect of Fe-dextran supplementation on antioxidant response

The transcription factor NF-κB plays a major role in coordinating innate and adaptive immunity, cellular proliferation, apoptosis and development, and it was proposed that it may be activated by $H_2O_2$ (Gloire et al., 2006). To determine if the changes in Fe and oxidative stress status described above are related to brain protection against injury, NF-κB levels were assessed in nuclear extracts from rat brains after 4 to 8 h of Fe-dextran administration (Fig. 4A) since total Fe content was increased over this period. A significant increase of 30% was detected after 8 h of Fe overload. Moreover, a consistent increased in the CAT activity was observed 21 h after Fe-dextran treatment (Fig. 4B).

### 3.5. Effect of Fe-dextran supplementation on isolated brain areas

Even though the increase of Fe concentrations in different parts of the brain could vary greatly due the different cellular characteristics in each area, Fe supplementation was found to alter Fe concentration in all tissues of the brain examined (Fig. 5). After 6 h of Fe administration Fe concentration in cortex, hippocampus and striatum was increased by 2.1-, 1.6- and 2.9-fold, respectively. Significant differences between Fe concentration in striatum and cortex (64%) and hippocampus and cortex (35%) were found. However, $LR^{\bullet}$ generation rate only increased significantly in brain cortex after Fe overload (2-fold) (Fig. 6). CAT activity was evaluated after Fe overload in each of the studied brain areas. Data in Table 2 show that the enzymatic activity significantly increased after 6 h of Fe administration only in cortex by 2.7-fold, and after 8 h of Fe

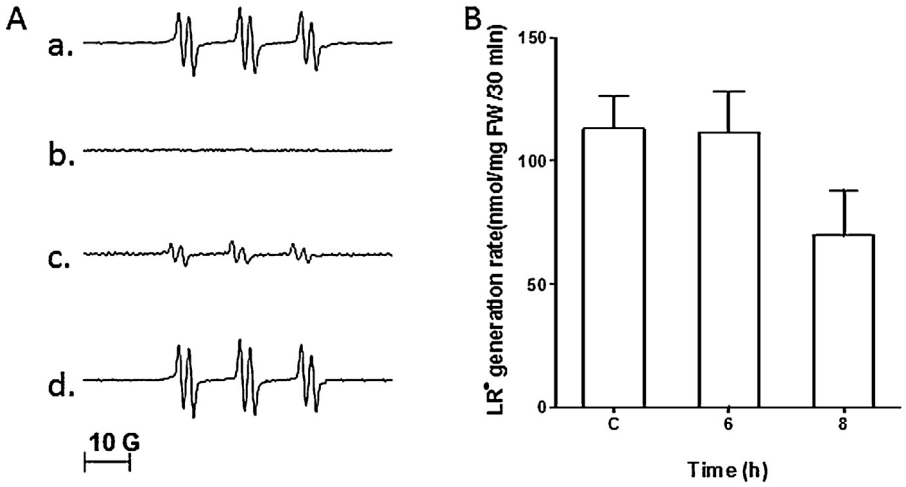


**Fig. 3.** LR• generation rate in rat brain. (A) EPR signal for LR• in control and Fe-overloaded rat brains, (a) computer simulated-spectrum employing the following spectral parameters: $g = 2.005$ and $a_{H^+} = 1.8$ G, (b) PBN-DMSO alone, (c) control rat brain, (d) Fe-overloaded rat brain at 6 h pi. (B) Kinetic study of LR• generation rate in rat brains after Fe administration. Brain homogenates were incubated in the presence of 40 mM PBN-DMSO for 30 min.

administration in cortex, hippocampus and striatum (1.4-fold, 85, and 46%, respectively).

## 4. Discussion

The results of this study showing the maximum increase in total Fe concentration in brain 6 h after Fe-dextran administration, gave coincidental information to that previously reported evidence that Fe status in the liver reached its maximum after 6 h employing an identical protocol of Fe supplementation (Puntarulo, 2005).

There is an increasing interest in the use of A• content in biological tissues as an informative, non-invasive, and natural indicator of oxidative stress (Roginsky and Stegmann, 1994). During its antioxidant action, $AH^-$ undergoes two consecutive one electron oxidations to dehydroascorbic acid (DHA) with intermediate formation of the A• (Hubel et al., 1997). A• has a relatively long half life time compared with other free radicals (approximately 50 s) (Buettner and Jurkiewicz, 1993) and it is easily detectable by EPR even at room temperature in aqueous solution. In contrast to A•, $AH^-$ and DHA are EPR silent (Hubel et al., 1997). In humans, enhancement in A• is associated with several oxidative stress conditions (Gey et al., 1987; Minakata et al., 1993; Pietri et al., 1994; Nakagawa et al., 1997; Courderot-Masuyer et al., 2000), including plasma from rats subjected to Fe overload *in vivo* (Galleano et al., 2002). $AH^-$ has a central metabolic role since it can act as an antioxidant and a pro-oxidant agent (Sadrzadeh and Eaton, 1988). Its pro-oxidant activity is the result of its ability to reduce metals (mainly Fe) to form species that react with $O_2$ to generate lipid peroxidation initiators (Wills and Epstein, 1966). $AH^-$ antioxidant activity is the result of its ability to reduce peroxyl radicals, propagating lipid peroxidation, or to reduce the oxidized form (α-tocopheroxyl radical) of the naturally occurring antioxidant α-T (Doba et al., 1985). Our results indicate a significant increase in the A•/$AH^-$ ratio at 6 h after Fe administration, indicating an oxidative stress condition temporally associated with the enhanced total Fe concentration of the brain.

The LIP, representing a minor fraction of the total cellular Fe (3–5%) (Kruszewski, 2003), is defined as a low-molecular-weight pool of weakly chelated Fe that rapidly passes through the cell, possibly consisting of both $Fe^{2+}$ and $Fe^{3+}$, associated with a variety of ligands with low affinity for Fe ions (Kakhlon and Cabantchik, 2002; Kruszewski, 2003). The accessibility of cellular Fe to chelators (such as DF) is commonly used as the criterion of 'lability'. It was also suggested that the LIP actually represents relatively weakly Fe bound

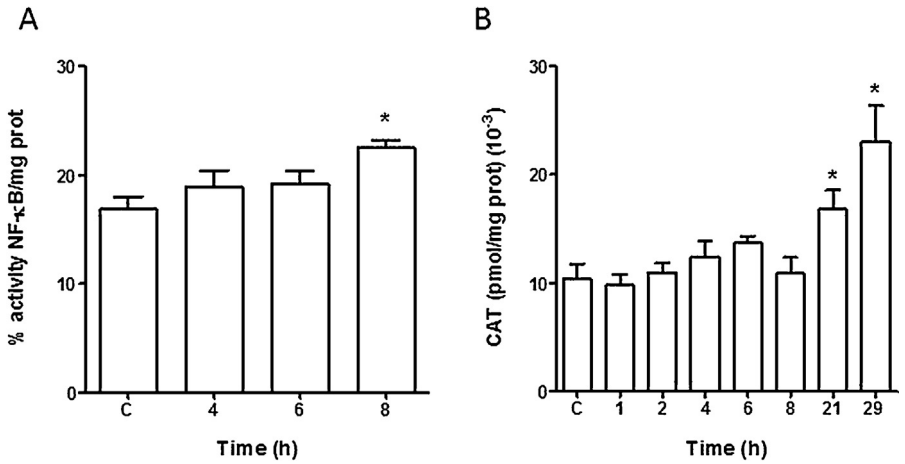


**Fig. 4.** NF-κB and CAT activities in rat whole brain. (A) Percentage of activity of NF-κB as a function of the Fe-overload time. (B) Kinetic study of CAT activity in rat brain. *Significantly different from control values, ANOVA, $p < 0.05$.

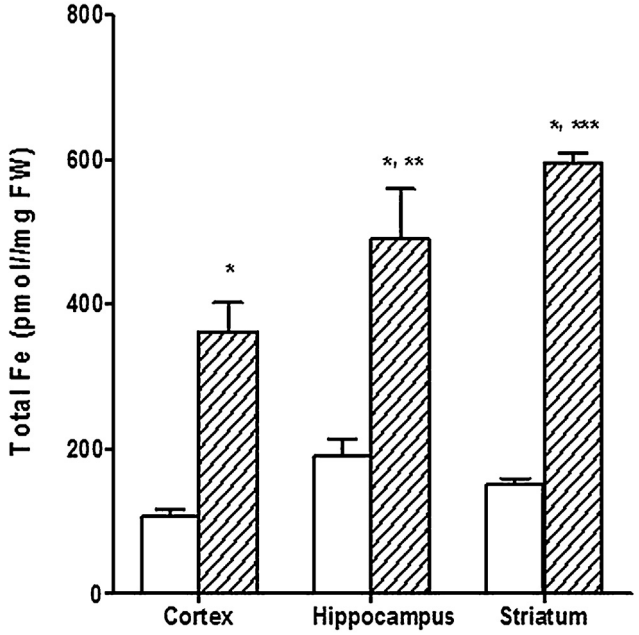


**Fig. 5.** Effect of Fe overload over the total Fe content in isolated brain areas. Fe content in control rat brains areas (□), and in indicated areas from brain samples isolated from Fe-overloaded rats 6 h pi (▨). *Significantly different from control values, ANOVA, $p < 0.05$. **Significantly different from cortex values after Fe treatment, ANOVA, $p < 0.1$. ***Significantly different from cortex values after Fe treatment, ANOVA, $p < 0.05$.

to prosthetic groups in functional sites of Fe-containing proteins, such as non-transferrin and non-ferritin (non-Ft) proteins, whose functions remain unknown (Petrák and Vyoral, 2001). Although our results indicate that the total Fe concentration in the brain returns to control values after 8–21 h post-Fe administration, the LIP concentration recovered control values after 8 h of Fe overload, an effect that may be related to Ft action. Ft plays a dual role in LIP homeostasis. In conditions of increased Fe deposits, Ft functions as Fe sequestering protein, protecting the cells against Fe toxicity. At low Fe conditions Ft acts as a source of Fe ions required

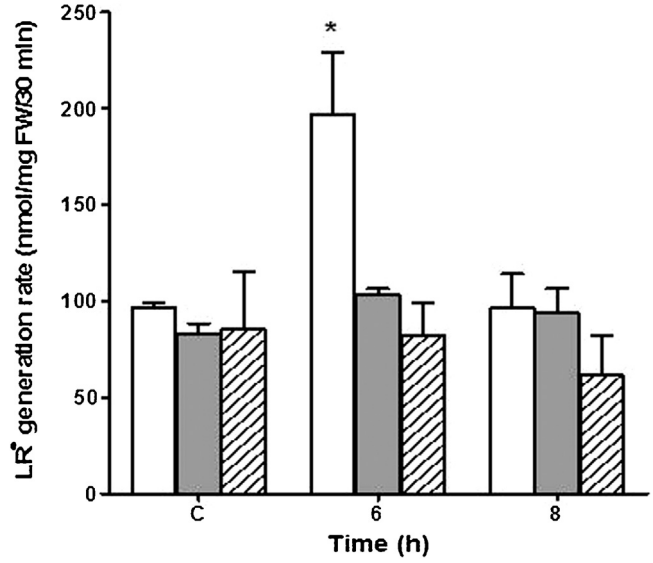


**Fig. 6.** Kinetic effect of Fe overload over the LR• generation rate in isolated brain areas. LR• generation rate in cortex (□), striatum (■) and hippocampus (▨) as a function of time after intraperitoneal administration of Fe-dextran. *Significantly different from control values, ANOVA, $p < 0.05$.

**Table 2**
CAT activity after Fe-dextran treatment in brain areas.

| | CAT activity (pmol/mg prot) ($10^{-3}$) |
|---|---|
| **Cortex** | |
| Control | 3.3 ± 0.3 |
| Fe-dextran 6 h | 9 ± 1* |
| Fe-dextran 8 h | 7.9 ± 0.7* |
| **Hippocampus** | |
| Control | 3.2 ± 0.5 |
| Fe-dextran 6 h | 4.1 ± 0.2 |
| Fe-dextran 8 h | 6.0 ± 0.6* |
| **Striatum** | |
| Control | 6.2 ± 0.3 |
| Fe-dextran 6 h | 3.5 ± 0.2 |
| Fe-dextran 8 h | 9 ± 1* |

* Significantly different from control values ($p < 0.05$).

for Fe-containing protein synthesis (Arosio and Levi, 2010). Thus, by the incorporation of excess Fe to the Ft, brain cells could be protected from the damage due to the increased ROS generation catalyzed by Fe contained in the LIP. The present results show that non-significant changes were detected in total brain, either in brain morphology or LR• production or TBARS content, 6 h after Fe administration. This new experimental evidence differs from the previous information in liver of animals subjected to the same protocol of Fe administration. Deterioration of the liver membranes, assessed as TBARS content, was significantly increased in the liver after 6 h of Fe-dextran injection, suggesting that lipid peroxidation, a key factor in hepatotoxicity, is not seen in brain homogenates. Even though the experiments presented here cannot ruled out the possibility that some of the effects observed in brain could be a consequence of Fe-dependent liver damage, the lack of a significant increase in total brain lipid peroxidation at the same time point where Fe content is showing its maximum in both organs, allows us to assume that Fe-dependent oxidative stress in the brain may be of a different nature of that developed in the liver (*e.g.* with an initial important contribution in the hydrophilic cellular environment).

Thus, other events may occur in relation to the triggering of regulatory and protective effects by Fe-dependent signaling processes, leading to significant prevention of brain injury associated with the Fe excess. Increased Fe concentration in the brain is related to NF-κB DNA binding capacity, which may contribute to limit ROS-dependent damage associated to Fe catalytic activity, by triggering an enhanced activity of the antioxidant enzyme CAT. Cells have developed antioxidant defenses, represented by antioxidant enzymes consuming superoxide anions (SOD-1, -2 and -3) or degrading $H_2O_2$ (catalase, glutathione peroxidases and peroxiredoxins) (Engelhardt, 1999; Rhee et al., 2003). Moreover, moderate levels of ROS may act as second messengers in signal transduction and gene regulation systems, which occurs in a variety of cell types and under several biological conditions such as cytokine, growth factors and hormone treatments, ion transport, transcription, neuromodulation and apoptosis (Hensley et al., 2000; Lander, 1997). It is now well established that $H_2O_2$ is the main ROS mediating cellular signaling due to its capacity to inhibit tyrosine phosphatases through oxidation of cysteine residues in their catalytic domain, which in turn activates tyrosine kinases and downstream signaling (Tonks, 2005; Aslan and Ozben, 2003). NF-κB was the first transcription factor shown to be redox-regulated (Schreck et al., 1991; Legrand-Poels et al., 1990), and the molecular mechanisms underlying its activation are cell-type specific (Gloire et al., 2006). Depending on the level of ROS, different redox-sensitive transcription factors are activated, and thus coordinating diverse biological responses. An intermediate amount of ROS triggers an inflammatory response through the activation of NF-κB and

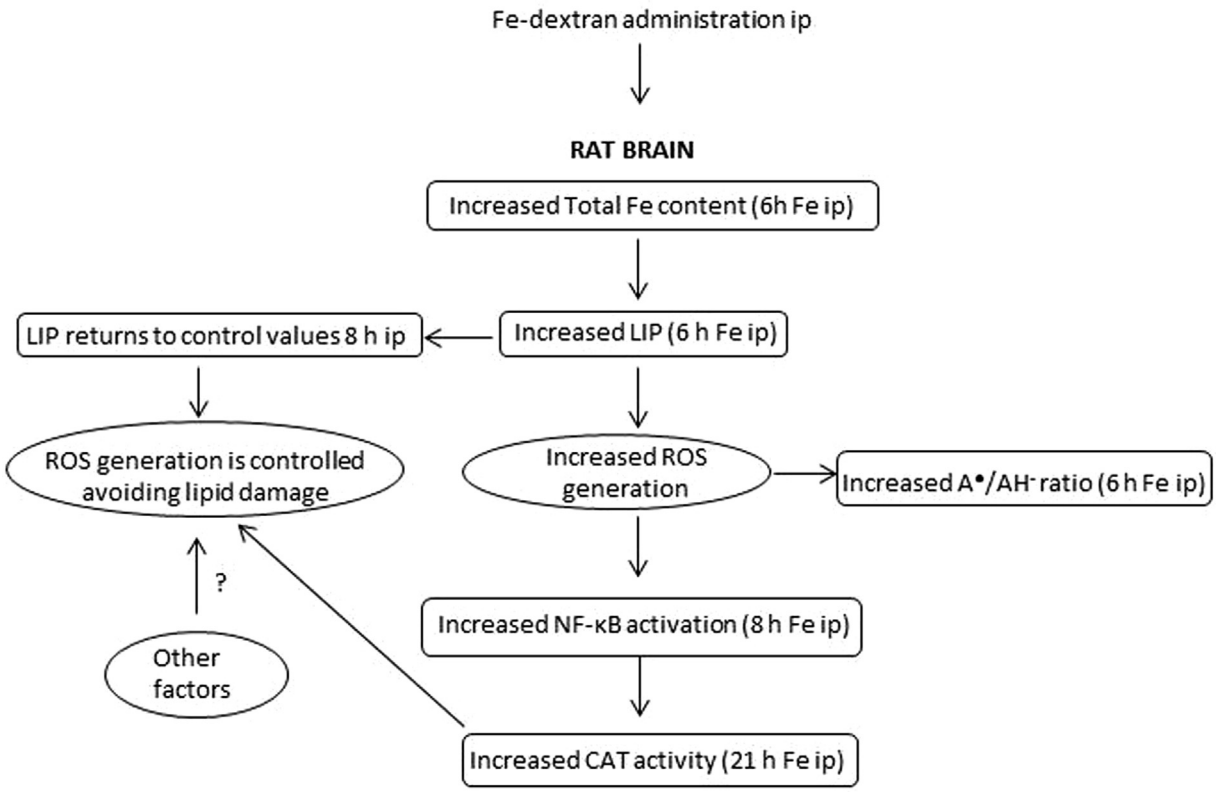


**Fig. 7.** Diagram showing a possible sequence of events occurring in the whole rat brain after Fe-dextran administration. Square framing corresponds to measured parameters.

AP-1 (Halliwell and Gutteridge, 1999). According to this hypothesis, the data shown here indicate a significant increase in NF-κB DNA binding activity after 8 h of Fe overload. This effect was followed by a significantly enhanced CAT activity after 21 h of Fe administration. A possible sequence of events, triggered by Fe overload in brain, is shown in Fig. 7. In agreement with this proposal, C57BL/6 mice supplemented with 3,5,5-trimethyl-hexanoil-ferrocene for 4 weeks exhibited significant increases in the hepatic expression of several antioxidant proteins including CAT and ferritin, which are categorized as nuclear factor erythroid 2-related factor 2 (Nrf2) target gene products (Moon et al., 2012). Similar to NF-κB, Nrf2 is a redox-sensitive transcription factor also affording protection against oxidative stress (Gloire et al., 2006), however, the influence of acute Fe administration on brain Nrf2 signaling requires further studies.

This scenario is in agreement with our results pointing out the lack of significant damage in the brain, and observations from clinical studies, showing no critical effects in human brains (Puntarulo, 2005). However, since Fe increased concentration lead to initial oxidative stress in the hydrophilic medium, it was postulated that Fe misregulation followed by an inadequate signaling-antioxidant response could be an initial cause of neuron death in some neurodegenerative diseases (Ke and Qian, 2007). However, this should be considered as an initial hypothesis that will require future experiments to assess if these events are part of the main route of the response mechanism to Fe overload in brain.

Moreover, the brain has multiple regions with specialized metabolic requirement and a variety of cell types with different Fe requirements. Lockman et al. (2012) showed variable susceptibility to Fe overload in endothelial, neuronal cells, and astrocytes in rats, by studying the response of calcium channels to voltage. Jiang et al. (2007) reported that chronic Fe overload may be more destructive to dopaminergic neurons in rat substantia nigra than the acute Fe overload. The striatum and the hippocampus are important structures in the brain and it was reported that they are associated with the development of Parkinson's and Alzheimer's disease (Wu et al., 2013). Our data clearly indicate that although Fe concentration increased in all the tested brain areas, Fe concentration in the striatum and hippocampus was more drastically enhanced than that in cortex. This observation could lead to the prediction that, if Fe-dependent damage appears, it will be located mostly in the striatum and hippocampus. Nevertheless, the comparison among the net increase in $LR^{\bullet}$ generation rate in the brain areas showed that lipid peroxidation in the cortex was significantly increased, $LR^{\bullet}$ remained unchanged after 6 h of Fe overload, in striatum and hippocampus samples. This information could be of interest from the clinical point of view, since it could be the key to understand why specific damage could occur. It seems that the cortex is more susceptible to oxidative stress conditions triggered by excess Fe, at the lipophilic level, than the rest of the tested areas. Either poor antioxidant capacity, different characteristics in the lipid composition, or a combination of both aspects could be responsible for the effect observed in the cortex, in relation to the other tested brain areas. Thus, the evaluation of Fe-dependent effects in brain should be taken with extreme caution to avoid underestimation of the complex mechanisms taking place when Fe overload is developed. A better understanding of all of these important aspects will greatly improve our knowledge of brain Fe metabolism as well as the role of its disruption in the development of neurodegenerative disorders.

## Acknowledgments

This study was supported by grants from the University of Buenos Aires, ANPCyT and CONICET to S.P: and FONDECYT 1110006 to V.F. S.P. is career investigator from CONICET, and N.P. is a fellow from CONICET.

## References


Aebi, H., 1984. Catalase in vitro. Methods Enzymol. 105, 121–126.

Arosio, P., Levi, S., 2010. Cytosolic and mitochondrial ferritins in the regulation of cellular iron homeostasis and oxidative damage. Biochim. Biophys. Acta 1800, 783–792.

Aslan, M., Ozben, T., 2003. Oxidants in receptor tyrosine kinase signal transduction pathways. Antioxid. Redox Signal. 5, 781–788.

Batista-Nascimento, L., Pimentel, C., Menezes, R.A., Rodrigues-Pousada, C., 2012. Iron and neurodegeneration: from cellular homeostasis to disease. Oxid. Med. Cell. Longev. 2012, 1–8.

Boveris, A.D., Puntarulo, S., 1998. Free-radical scavenging actions of natural antioxidants. Nutr. Res. 18, 1545–1557.

Brumby, P.E., Massey, V., 1967. Determination of nonheme iron, total iron and cooper. Methods Enzymol. 10, 463–474.

Buettner, G.R., 1987. Spin trapping: ESR parameters of spin adducts. Free Radic. Biol. Med. 3, 259–303.

Buettner, G.R., Jurkiewicz, B.A., 1993. Ascorbate free radical as a marker of oxidative stress: an EPR study. Free Radic. Biol. Med. 14, 49–55.

Chen, G., Jing, C.H., Liu, P.P., Ruan, D., Wang, L., 2013. Induction of autophagic cell death in the rat brain caused by iron. Am. J. Med. Sci. 345, 369–374.

Courderot-Masuyer, C., Lahet, J.J., Verges, B., Brun, J.M., Rochette, L., 2000. Ascorbyl free radical release in diabetic patients. Cell. Mol. Biol. 46, 1397–1401.

Czerniczyniec, A., Karadayian, A.G., Bustamante, J., Cutrera, R.A., Lores-Arnaiz, S., 2011. Paraquat induces behavioral changes and cortical and striatal mitochondrial dysfunction. Free Radic. Biol. Med. 51, 1428–1436.

Darbari, D., Loyevsky, M., Gordeuk, V., Kark, J.A., Castro, O., Rana, S., 2003. Fluorescence measurements of the labile iron pool of sickle erythrocytes. Blood 102, 357–364.

Deryckere, F., Gannon, F., 1994. A one-hour minipreparation technique for extraction of DNA-binding proteins from animal tissues. Biotechniques 16, 405.

Desai, I., 1984. Vitamin E analysis methods for animal tissues. Methods Enzymol. 105, 138–146.

Doba, T., Burton, G.W., Ingold, K.U., 1985. Antioxidant and co-antioxidant activity of vitamin C. The effect of vitamin C, either alone or in the presence of vitamin E or a water soluble vitamin E analogue, upon the peroxidation of aqueous multilamellar phospholipid liposomes. Biochim. Biophys. Acta 835, 298–303.

Engelhardt, J.F., 1999. Redox-mediated gene therapies for environmental injury: approaches and concepts. Antioxid. Redox Signal. 1, 5–27.

Floyd, R.A., Carney, J.M., 1992. Free radical damage to protein and DNA: mechanisms involved and relevant observations on brain undergoing oxidative stress. Ann. Neurol. 32 (Suppl.), S22–S27.

Galleano, M., Puntarulo, S., 1992. Hepatic chemiluminescence and lipid peroxidation in mild iron overload. Toxicology 76, 27–38.

Galleano, M., Puntarulo, S., 1994. Effect of mild iron overload on liver and kidney lipid peroxidation. Braz. J. Med. Biol. Res. 27, 2349–2358.

Galleano, M., Puntarulo, S., 1995. Role of antioxidants on the erythrocytes resistance to lipid peroxidation after acute iron overload in rats. Biochim. Biophys. Acta 1271, 321–326.

Galleano, M., Aimo, L., Puntarulo, S., 2002. Ascorbyl radical/ascorbate ratio in plasma from iron overloaded rats as oxidative stress indicator. Toxicol. Lett. 133, 193–201.

Galleano, M., Simontacchi, M., Puntarulo, S., 2004. Nitric oxide and iron: effect of iron overload on nitric oxide production in endotoxemia. Mol. Aspects Med. 25, 141–154.

Gerlach, M., Ben-Shachar, D., Riederer, P., Youdin, M., 1994. Altered brain metabolism of iron as a cause of neurodegenerative diseases? J. Neurochem. 63, 793–807.

Gey, K.F., Stähelin, H.B., Puska, P., Evans, A., 1987. Relationship of plasma level of vitamin C to mortality from ischemic heart disease. Ann. N. Y. Acad. Sci. 498, 110–123.

Gloire, G., Legrand-Poels, S., Piette, J., 2006. NF-kB activation by reactive oxygen species: fifteen years later. Biochem. Pharmacol. 72, 1493–1505.

Halliwell, B., 2006. Oxidative stress and neurodegeneration: where are we now? J. Neurochem. 97, 1634–1658.

Halliwell, B., Gutteridge, J.M.C., 1984. Oxygen toxicity, oxygen radicals, transition metals and disease. Biochem. J. 219, 1–14.

Halliwell, B., Gutteridge, J., 1999. Free Radicals in Biology and Medicine, third ed. Clarendon Press, Oxford, UK.

Hensley, K., Robinson, K.A., Gabbita, S.P., Salsman, S., Floyd, R.A., 2000. Reactive oxygen species, cell signaling, and cell injury. Free Radic. Biol. Med. 28, 1456–1462.

Hubel, C.A., Kagan, V.E., Kisin, E.R., McLaughlin, M.K., Roberts, J.M., 1997. Increased ascorbate radical formation and ascorbate depletion in plasma from women with preeclampsia: implications for oxidative stress. Free Radic. Biol. Med. 23, 597–609.

Jiang, H., Song, N., Wang, J., Ren, L.Y., Xie, J.X., 2007. Peripheral iron dextran induced degeneration of dopaminergic neurons in rat substantia nigra. Neurochem. Int. 51, 32–36.

Jurkiewicz, B.A., Buettner, G.R., 1994. Ultraviolet light-induced free radical formation in skin: an electron paramagnetic resonance study. Photochem. Photobiol. 59, 1–4.

Kakhlon, O., Cabantchik, Z.I., 2002. The labile iron pool: characterization, measurement, and participation in cellular processes (1). Free Radic. Biol. Med. 33, 1037–1046.

Ke, Y., Qian, Z.M., 2007. Brain iron metabolism: neurobiology and neurochemistry. Prog. Neurobiol. 83, 149–173.

Kotake, Y., Tanigawa, T., Tanigawa, M., Ueno, I., Randel Allen, D., Lai, C.S., 1996. Continuous monitoring of cellular nitric oxide generation by spin trapping with an iron dithiocarbamate complex. Biochim. Biophys. Acta 1289, 362–368.

Kruszewski, M., 2003. Labile iron pool: the main determinant of cellular response to oxidative stress. Mutat. Res. 531, 81–92.

Kutnink, M.A., Hawkes, W.C., Schaus, E.E., Omaye, S.T., 1987. An internal standard method for the unattended high-performance liquid chromatographic analysis of ascorbic acid in blood components. Anal. Biochem. 166, 424–430.

Lai, E.K., Crossley, C.R., Sridhar, H.P., Misra, E.G., Janzen McCay, P.B., 1986. In vivo spin trapping of free radicals generated in brain, spleen, and liver during γ radiation of mice. Arch. Biochem. Biophys. 244, 156–160.

Lander, H.M., 1997. An essential role for free radicals and derived species in signal transduction. FASEB J. 11, 118–124.

Laurie, S.H., Tancock, N.P., McGrath, S.P., Sanders, J., 1991. Influence of complexation on the uptake by plants of iron, manganese, copper and zinc: I. Effect of EDTA in a multimetal and computer simulation study. Exp. Bot. 42, 509–513.

Legrand-Poels, S., Vaira, D., Pincemail, J., van de Vorst, A., Piette, J., 1990. Activation of human immunodeficiency virus type 1 by oxidative stress. AIDS Res. Hum. Retroviruses 6, 1389–1397.

Lockman, J.A., Geldenhuys, W.J., Bohn, K.A., Desilva, S.F., Allen, D.D., Van der Schyf, C.J., 2012. Differential effect of nimodipine in attenuating iron-induced toxicity in brain- and blood-brain barrier-associated cell types. Neurochem. Res. 37, 134–142.

Lowry, O.H., Rosebrough, N.J., Farr, A.L., Randall, R.J., 1951. Protein measurement with the Folin phenol reagent. J. Biol. Chem. 193, 265–275.

Maaroufi, K., Ammari, M., Jeljeli, M., Roy, V., Sakly, M., Abdelmelek, H., 2009. Impairment of emotional behavior and spatial learning in adult Wistar rats by ferrous sulfate. Physiol. Behav. 96, 343–349.

Maaroufi, K., Save, E., Poucet Sakly, B., Abdelmelek, H., Had-Aissouni, L., 2011. Oxidative stress and prevention of the adaptive response to chronic iron overload in the brain of young adult rats exposed to a 150 kilohertz electromagnetic field. Neuroscience 186, 39–47.

Minakata, K., Suzuki, O., Saito, S., Harada, N., 1993. Ascorbate radical levels in human sera and rat plasma intoxicated with paraquat and diquat. Arch. Toxicol. 67, 126–130.

Moon, M.S., McDevitt, E.I., Zhu, J., Stanley, B., Krzeminskym, J., Amin, S., Aliaga, C., Miller, T.G., Isom, H.C., 2012. Elevated hepatic iron activates NF-E2-related factor2-regulated pathway in a dietary iron overload mouse model. Toxicol. Sci. 129, 74–85.

Nakagawa, K., Kanno, H., Miura, Y., 1997. Detection and analyses of ascorbyl radical in cerebrospinal fluid and serum of acute lymphoblastic leukemia. Anal. Biochem. 254, 31–35.

Papanastasiou, D.A., Vayenas, D.V., Vassilopoulos, A., Repanti, M., 2000. Concentration of iron and distribution of iron and transferrin after experimental iron overload in rat tissues in vivo: study of the liver, the spleen, the central nervous system and other organs. Pathol. Res. Pract. 196, 47–54.

Pardridge, W.M., Eisenberg, J., Yang, J., 1987. Human blood–brain barrier transferrin receptor. Metabolism. 36, 892–895.

Petrák, J.V., Vyoral, D., 2001. Detection of iron-containing proteins contributing to the cellular labile iron pool by a native electrophoresis metal blotting technique. J. Inorg. Biochem. 86, 669–675.

Pietri, S., Culcasi, M., Albat, B., Albérici, G., Menasché, P., 1994. Direct assessment of the antioxidant effects of a new heart preservation solution, Celsior. A hemodynamic and electron spin resonance study. Transplantation 58, 739–742.

Piloni, N., Puntarulo, S., 2010. Iron role in the oxidative metabolism of animal and plant cells. Effect of iron overload. In: Gimenez, M.S. (Ed.), Metals in Biology Systems, Research Signpost. Transworld Research Network, Trivandrum, Kerala, India, pp. 29–50.

Puntarulo, S., 2005. Iron, oxidative stress and human health. Mol. Aspects Med. 26, 299–312.

Rhee, S.G., Chang, T.S., Bae, Y.S., Lee, S.R., Kang, S.W., 2003. Cellular regulation by hydrogen peroxide. J. Am. Soc. Nephrol. 14, S211–S215.

Robello, E., Galatro, A., Puntarulo, S., 2007. Iron role in oxidative metabolism of soybean axes upon growth: effect of iron overload. Plant Sci. 172, 939–947.

Roginsky, V.A., Stegmann, H.B., 1994. Ascorbyl radical as natural indicator of oxidative stress: quantitative regularities. Free Radic. Biol. Med. 17, 93–103.

Sadrzadeh, S.M., Eaton, J.W., 1988. Hemoglobin-mediated oxidant damage to the central nervous system requires endogenous ascorbate. J. Clin. Invest. 82, 1510–1515.

Schreck, R., Rieber, P., Baeuerle, P.A., 1991. Reactive oxygen intermediates as apparently widely used messengers in the activation of the NF-kappa B transcription factor and HIV-1. EMBO J. 10, 2247–2258.

Tapia, G., Troncoso, P., Galleano, M., Fernández, V., Puntarulo, S., Videla, L.A., 1998. Time course study of the influence of acute iron overload on Kupffer cell functioning and hepatotoxicity assessed in the isolated perfused rat liver. Hepatology 27, 1311–1316.

Tonks, N.K., 2005. Redox redux: revisiting PTPs and the control of cell signalling. Cell 121, 667–670.

Vázquez, R., Riveiro, M.E., Mondillo, C., Perazzo, J.C., Vermeulen, M., Baldi, A., Davio, C., Shayo, C., 2013. Pharmacodynamic study of the 7,8-dihydroxy-4-methylcoumarin-induced selective cytotoxicity toward U-937 leukemic cells versus mature monocytes: cytoplasmic p21(Cip1/WAF1) as resistance factor. Biochem. Pharmacol. 86, 210–221.

Wills, E.J., Epstein, M.A., 1966. Subcellular changes in surface adenosine triphosphatase activity of human liver in extrahepatic obstructive jaundice. Am. J. Pathol. 49, 605–635.
Wu, J., Ding, T., Sun, J., 2013. Neurotoxic potential of iron oxide nanoparticles in the rat brain striatum and hippocampus. Neurotoxicology 34, 243–253.
Yu, S., Feng, Y., Shen, Z., Li, M., 2011. Diet supplementation with iron augments brain oxidative stress in a rat model of psychological stress. Nutrition 27, 1048–1052.
Zheng, W., Monnot, A.D., 2012. Regulation of brain iron and copper homeostasis by brain barrier systems: implication in neurodegenerative diseases. Pharmacol. Ther. 133, 177–188.